Vol. 40, No. 4 (2018) 633-642, DOI: 10.24874/ti.2018.40.04.10

Tribology in Industry

www.tribology.rs

RESEARCH

Optimization of Three Body Abrasive Wear Behaviour of Stir Cast A356/ $ZrSiO_4$ Metal Matrix Composite

T. Satish Kumar[a], R. Raghu[b], K. Krishna Kumar[a], S. Shalini[c], R. Subramanian[a]

[a]*Department of Metallurgical Engineering, PSG College of Technology, Coimbatore-641004, Tamilnad, India,*
[b]*Department* of *Mechanical Engineering, Sri Ramakrishna Engineering College, Coimbatore-641022, Tamilnadu India*
[c]*Department of Physics, PSG College of Technology, Coimbatore-641004, Tamilnadu, India.*

Keywords:

Metal Matrix Composite
$ZrSiO_4$ particles
Three body abrasive wear
Response Surface Methodology
Analysis of Variance

Corresponding author:

T.Satish Kumar
Department of Metallurgical Engineering, PSG College of Technology, Coimbatore-641004, Tamilnadu.
E-mail: satishmetly@gmail.com

A B S T R A C T

In the current research, abrasive wear of A356/15 wt% $ZrSiO_4$ metal matrix composite has been investigated. Microstructural analysis of the fabricated composites revealed that $ZrSiO_4$ particles were uniformly distributed in the matrix. Response Surface Methodology adopted for designing abrasive wear experiments using different parameters such load, speed and time. Experiments were performed using a dry abrasion tester. Surface plots were generated for the interaction of different parameters with the abrasive wear rate. Surface plots show that the wear rate tends to increase with increasing load and sliding distance while it decreases as the speed increases. Regression analysis result in a good relation of the parameters with the wear rate which confirm the accuracy of the model developed. Moreover, the optimal combination of the testing parameters which result in low abrasion wear rate is determined.

1. INTRODUCTION

In the recent decades, usage of Aluminum Metal Matrix Composites (AMMCs) has increased significantly in several applications owing to its better wear properties, higher specific strength, high stiffness and lower coefficient of thermal expansion compared to that of unreinforced aluminium alloy [1-3].Several authors have reported that incorporation of the ceramic particles such as Boron, Silicon Nitride, Silica Sand, Magnesium Oxide, Mica, Glass Beads, Boron Nitride, Silicon Carbide, Titanium Carbide, Alumina, Titanium Boride and Boron Carbide in the Al matrix tends to enhance the mechanical properties [4-6]. Among the various ceramic reinforcements, Zircon ($ZrSiO_4$) has been identified as a potential candidate with exceptional characteristics such as high elastic modulus, better hardness and high thermal stability. Zircon also offers very low thermal expansion coefficient when compared to other ceramic materials [4,7]. Several technologies have been adopted for fabricating the AMMCs including squeeze casting, stir casting, powder metallurgy, compo-casting, spray forming, in-situ

casting, liquid metal infiltration and mechanical alloying [2]. Difficulties associated with the fabrication of the AMMCs include attainment of uniform dispersion of the reinforcement particles, wettability between the reinforcement and the molten metal, agglomeration of the reinforcements, porosity formation and chemical reactions between the matrix and the reinforcement during processing of the composites. However, stir casting process is the simplest, economical process which offering a uniform distribution and a good bonding of the reinforcements with the matrix [8,9].

Sharma et al. [10] studied dry sliding wear behavior of the Al6082/graphite composites using Response Surface Methodology (RSM) and investigated the influence of wear parameters such as load, speed and sliding distance. They reported that sliding distance had the highest influence on the wear rate of the composites while the load had the least effect on the wear rate. Radhika and SaiCharan [11] investigated three body abrasion of the TiC (10 wt%) reinforced Al LM25 MMC (Metal Matrix Composite) using RSM. Wear analysis was carried out as a function of wear parameters. Optimization of the wear parameters was also done. Results revealed that a minimum wear rate of 0.00104 mm^3/Nm was obtained under an optimum load of 27 N, speed of 139 rpm and time of 3 min. Kaushik and Rao [12] evaluated two body abrasive wear behavior of hybrid Al6082/SiC/Gr composites under control conditions, load in the range of 5–15 N, grit sizes in the range of 100 μm – 200 μm with constant sliding distance of 75 m. As cast and T6 heat treated Al–SiC–Gr composite exhibited an increase of 16.4 % and 27 % in wear resistance at an applied load of 15 N and grit size of 200 μm. It was also reported that wear resistance improved at constant load as the grit size decreased.

Natarajan et al. [13] studied the dry sliding wear behavior of Al 6061 hybrid metal matrix composites reinforced with fly ash (3, 6 and 9 wt%) and graphite (fixed 3 wt%), and determined that 9.81 N load, 4 m/s speed and 9 wt% fly ash resulted in minimum wear rate. Kok [14] interpreted that the factors such as grain size of abrasive, counterface hardness and reinforcement phase has significant influence over the dry sliding wear behavior of aluminium alloy based composites. Singh et al. [15] investigated on optimization of wear parameters of Al 2025/3wt. % Al_2O_3/3wt. % graphite/1wt% B_4C hybrid MMCs using Taguchi technique. From the results, it is observed that applied load has highest contribution on the followed by the sliding distance.Radhika [16] studied the three body abrasive wear behaviour of centrifugally cast aluminium/Ni coated SiC composite through taguchi technique. Results revealed that radial distance as the first significant factor having contribution on the wear rate (40.59 %), subsequently followed by load with 29.7 % and speed with 14.85 %).Radhika and Raghu [17] compared the three body abrasive wear behavior of functionally graded MMCs with the homogenous composites (Al/AlN and Al/SiO_2-10 wt%). From the results, it is concluded that outer surface of the Al/AlN FGM exhibited greater wear resistance at all parametric conditions compared to the homogenous composites and monolithic alloy.

From the literature survey, it was observed that the three body abrasion behavior of $ZrSiO_4$ particulate reinforced AMMC has not been investigated. Hence in the current research, an attempt has been made to prepare Aluminum A356/$ZrSiO_4$ MMC through stir casting and to investigate its three body abrasive wear behavior using RSM.

2. MATERIALS AND METHODS

A356alloy was selected as the matrix as it is extensively used in automotive applications such as cylinder heads, cylinder blocks and transmission cases. It is also used in aircraft structures and nuclear reactor components requiring high strength. This alloy also possesses very good castability, weldability and enhanced corrosion resistance. $ZrSiO_4$ particles (Fig. 1) were chosen as reinforcement for incorporation in to A356 alloy for enhancing the wear resistance.

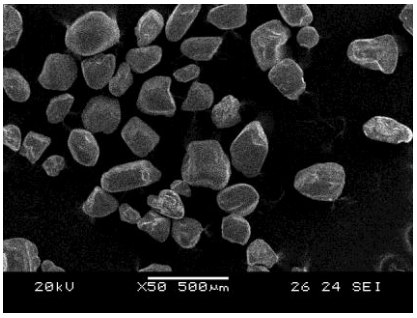

Fig. 1. Morphology of $ZrSiO_4$ particles.

Table1. Chemical composition of the A356 alloy.

A356 alloy	Si	Fe	Cu	Mn	Mg	Zn	Ni	Al
wt%	7.5	0.3	0.2	0.3	0.6	0.1	0.1	90.9

$ZrSiO_4$ particles were examined using Scanning Electron Microscope to observe the morphology and size distribution. It was observed that the zircon particles were irregular and angular in shape. The densities of the alloy and the reinforcement were 2.685 g/cm^3 and 4.23 g/cm^3 respectively. Chemical composition of the A356 alloy was checked through Optical Emission Spectrometer (OES) and shown in Table 1.

2.1 Fabrication of composite

A356 aluminum alloy was taken and loaded into the graphite crucible for the melting purpose. The loaded crucible was kept inside the electrical resistance furnace and allowed to melt. The zircon particles were preheated (400 °C) in order for removal of moisture to promote wettability of the reinforcement by the molten aluminum alloy. Once the aluminum was melted, the preheated particles were introduced into the molten metal through the hopper and simultaneous stirring of the molten metal was carried out using the stirrer. This stirrer was rotated with the aid of motor and it helps in uniform dispersion of reinforcement particles in the molten metal. The stirring speed during synthesizing of the composites was maintained at 300 rpm and the temperature during entire addition was maintained as 750 °C. This stirring speed is preferred in order to avoid agglomeration and to promote dispersion of the particulates uniformly in the viscous melt. After addition of the reinforcement particles, the molten metal was taken out and poured into the die (carbon steel) with dimensions of 30×90×15 mm. The cast part was ejected from the die after complete solidification of the composite.

2.2 Microstructural characterization

Composite and unreinforced alloy specimens were polished using belt polisher. Then it was polished using emery sheets and disc polisher with diluted alumina (powders of size 100 nm) solution. Prior to observation, the specimens were etched using the Keller's reagent (95 mL water, 2.5 mL HNO_3, 1.5 mL HCl, 1.0 mL HF) and it was observed under an optical microscope (Eclipse MA-100, Nikon).

2.3 Abrasive wear test

Figure 2 shows the equipment of dry abrasion tester used in the present study. Abrasive wear behavior of composites was carried out according to standard ASTM G65-16.

Fig. 2. Dry abrasion tester.

The rectangular specimen with dimensions of about 25x76x10 mm was machined from as cast sample. Dry abrasion equipment consisting of a 250 mm diameter chlorobutyl rubber wheel and speed range of 1 to 300 rpm was used in the current study. Specimen can be hold against the rotating wheel by loading the lever attached to the specimen holder. This load tends to keep the specimen in contact with the rubber wheel. Silica sand of size AFS 50/70 (200 μm) was used as an abrasive medium loaded in a hopper. The loaded abrasive medium was allowed to fall between the specimen and the rotating wheel through the nozzle at the constant flow rate of 354 g/min (for all test conditions) and gets collected at the bottom of the tester where the abrasive medium collector was kept.The three body abrasive wear experiments were carried out for the different condition of applied load (10-50 N), rotating speed of wheel (50-150 rpm) and sliding distance (117-589 m). The parameters and their levels considered for performing the experiments were given in Table 2. Central Composite Design (CCD) under RSM was preferred for designing the experiments using the statistical software Minitab. Prior to abrasion test, the specimens were measured for its weight and also measured after completion of test. The difference in the weight of the specimens is used for calculation of abrasion

wear rate of the composite. The abrasion wear rate is given by Eq. (1) [11] .

$$W = \frac{\Delta G}{dMS} \quad (1)$$

where W is the abrasion wear rate, ΔG is the weight loss, d is the density of the composite, M is the applied load and S is the sliding distance.

2.4 Response surface methodology

RSM is a powerful statistical technique which is employed for analysis and developing of model with less number of experiments. For the selected parametric conditions as given in Table 2, the Design table is generated with 20 experimental runs, presented in Table 3. The abrasion wear rate obtained through the experiments will be analyzed for studying the significance of the parameters.

Table 2. Parametric levels considered for Designing of Experiments (DOE).

Level	Load (N)	Speed (rpm)	Sliding distance (m)
1	10	0.5	117
2	15	75	235
3	20	100	353
4	25	125	471
5	30	150	589

3. RESULTS AND DISCUSSION

The micro structural examination, abrasion wear rate and wear mechanisms of the A356/$ZrSiO_4$ has been discussed in detail.

3.1 Microstructural examination

Optical microstructures of the monolithic A356 alloy and the composites are shown in Figs. 3a and 3b respectively. Figure 3a reveals that the silicon particles are present at the interdendritic region of the α-Aluminum matrix. Figure 3b reveals that the $ZrSiO_4$ particles (grey) are uniformly distributed in the aluminum matrix which is attributed to the optimum stirring speed and time maintained during synthesizing of the composites. It was also observed that significant refinement of dendritic arm in the composites is resulted compared to that of the matrix alloy which can be attributed to the heterogeneous nucleation effect resulting from the addition of $ZrSiO_4$ particles [7]. Measurement of aspect ratio of dendritic arms was carried out using image analyzer software. The primary α-Al dendrite as observed from the microstructure of A356 alloy (Fig. 3a) appears elongated with aspect ratio of 4.90. Whereas, the composite sample aspect ratio was 3.78. Similar type of findings has been reported by Nampoothiri et al. [18] in A356/TiB_2 system.

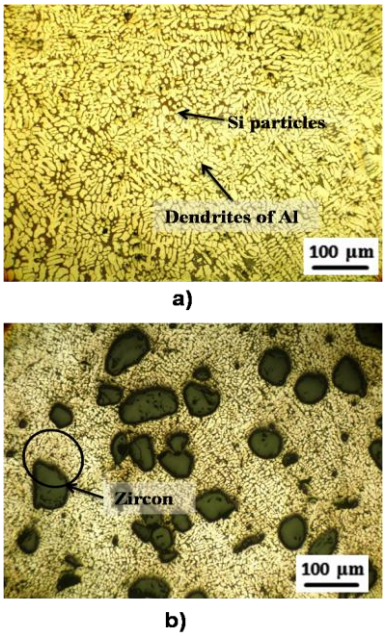

Fig. 3. Micro structural features of (a) A356 alloy and (b) A356/$ZrSiO_4$composite.

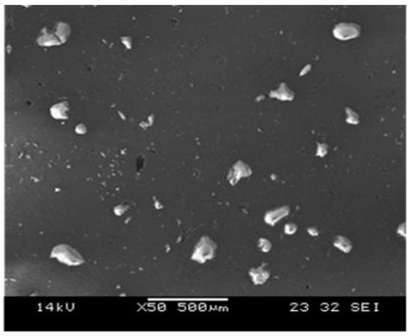

Fig. 4. SEM image of A356alloy /$ZrSiO_4$ composite.

Figure 4 shows theSEM image of A356alloy /15 wt% $ZrSiO_4$ reinforced composite. It reveals the uniform distribution of $ZrSiO_4$ particles in A356 aluminium alloy matrix (Fig. 4). There is no evidence of voids at the particle matrix interface, indicating a strong continuous bond between zircon particle and the alloy matrix.

3.2 XRD analysis

X-ray diffraction pattern of A356 alloy MMCs reinforced with 15 wt% of zircon is shown in Fig. 5.

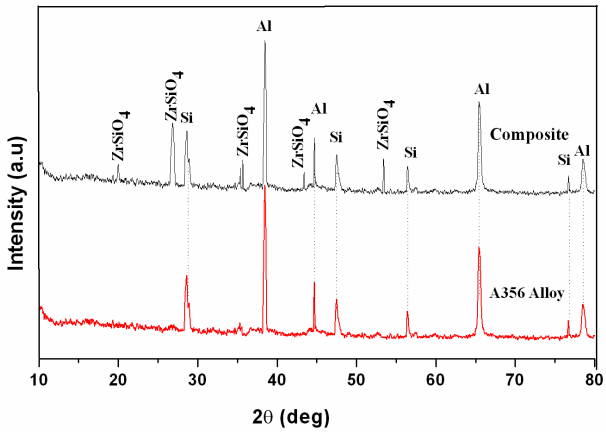

Fig. 5. X-ray diffraction pattern for the A356 alloy and composites.

XRD pattern revealed the presence of Al, Si and $ZrSiO_4$. There is no evidence of formation secondary phases.

3.3 Abrasion wear behavior of the A356/$ZrSiO_4$ composite

The obtained abrasion wear rates for the different parametric condition of the experimental design are displayed in Table 3. These results are analysed through the statistical software Minitab.

Table 3. Wear rates obtained from three body abrasions testing of composite.

S.No	Load (N)	Speed (rpm)	Sliding Distance (m)	Wear rate (mm^3/Nm)
1	20	50	353	0.00190
2	25	75	471	0.00219
3	20	100	353	0.00149
4	25	125	235	0.00119
5	20	100	353	0.00150
6	25	70	235	0.00210
7	20	100	353	0.00149
8	15	75	235	0.00124
9	15	75	471	0.00147
10	20	100	353	0.00149
11	15	125	471	0.00109
12	20	100	589	0.00170
13	30	100	353	0.00224
14	20	100	353	0.00149
15	10	100	353	0.00107
16	20	150	353	0.00156
17	20	100	353	0.00149
18	20	100	117	0.00136
19	25	125	471	0.00211
20	15	125	235	0.00114

3.4 Regression model and confirmation experiments

The regression model is generated using RSM based on the obtained abrasion wear rates (Eq. 2). The obtained R^2 (91.89 %) and adj R^2 (84.59 %) are found closer to each other which evident that the quadratic model developed can predicting the wear rate effectively based on the input parameters.

$$\text{Wear rate } (mm^3/Nm) = 0.000607 + 0.000057\,L - 0.000005\,S + 0.000001\,SD \quad (2)$$

where L is the load in N, S is the wheel speed in rpm and SD is the sliding distance in m.

Regression model shows that wear rate is a function of constant, linear and square terms. The term prefixed with positive sign indicates that an increase in the wear rate as the parameters involved while a negative sign denotes that the parameter involved significantly decreases the wear rate.

3.5 Model validation

The accuracy of the resulted model is checked by conducting the confirmation abrasion wear experiments. These confirmation experiments are conducted using new set of parameters other than the condition obtained in the CCD design table. The similar conditions are also substituted in the model Eq. (2) to obtain the abrasion wear rate theoretically. The obtained wear rates from experiments and the model are used for calculating the deviation of the model in predicting the wear rates (Table 4). The error between the abrasion wear rates is less than 5 % which indicates that developed model is adequate enough to predict the wear behavior of the composite.

3.6 Analysis of variance

Analysis of Variance (ANOVA) was performed for a confidence level of 95 % to estimate the percentage significance of the wear process parameters on the abrasion wear rate of the composites (Table 5). Table 5, shows the significance of the linear, square, interaction terms as well as the lack of fit. For a confidence level of 95 %, the standard F value is 5.0. The F value of lack of fit should be lesser than this value for the model to be adequate.

Table 4. Comparison of model and experimental abrasion wear rates.

Exp No	Load (N)	Speed (rpm)	Sliding distance (m)	Experiment Wear rate (mm^3/Nm)	Predicted Wear rate (mm^3/Nm)	Error (%)
1	13	60	175	0.00128	0.00122	4.6
2	22	115	420	0.00175	0.00170	2.8
3	28	140	540	0.00212	0.00204	3.7

Table 5. ANOVA for abrasion wear rate of the composite.

Source	DF	Seq SS	Adj SS	Adj MS	F-value	P-value	Contribution (%)
Model	9	0.000002	0.000002	0.000000	12.59	0.000	91.89
Linear	3	0.000002	0.000002	0.000001	33.86	0.000	82.41
Load	1	0.000002	0.000002	0.000002	75.75	0.000	61.45
Speed	1	0.000000	0.000000	0.000000	14.81	0.003	12.01
Sliding distance	1	0.000000	0.000000	0.000000	11.03	0.008	8.95
Square	3	0.000000	0.000000	0.000000	1.37	0.309	3.32
Load *Load	1	0.000000	0.000000	0.000000	1.16	0.308	0.70
Speed *Speed	1	0.000000	0.000000	0.000000	3.15	0.106	2.61
Sliding distance *Sliding distance	1	0.000000	0.000000	0.000000	0.01	0.927	0.01
2-Way Interaction	3	0.000000	0.000000	0.000000	2.53	0.116	6.16
Load *Speed	1	0.000000	0.000000	0.000000	1.58	0.238	1.28
Load *Sliding distance	1	0.000000	0.000000	0.000000	4.18	0.068	3.39
Speed *Sliding distance	1	0.000000	0.000000	0.000000	1.83	0.205	1.49
Error	10	0.000000	0.000000	0.000000			8.11
Lack-of-Fit	5	0.000000	0.000000	0.000000	2.52	0.345	8.11
Pure Error	5	0.000000	0.000000	0.000000			0.00
Total	19	0.000003					100.00

The obtained F value of lack of fit is 2.52 which indicate that the model is accurate enough to in predict the abrasive wear behavior of the composite. Among the variety of parameters, load is found to be the dominant parameter having percentage significance of 61.45 % followed by speed (12.01 %) and sliding distance (8.95 %). This is evident from the P value since the P value must be lesser than 0.05 for the parameter to have greater influence on the wear rate. From the Table 5, it is ensured that the load has the lesser P-value of 0.000 compared to that of the speed (0.003) and sliding distance (0.008).

3.7 Significance of the wear process parameters on abrasion wear rate

Surface plots were constructed based on the results obtained for the different combination of the parameters (Fig. 6). From these plots, the variation of abrasion wear rate with respect to variation in the parametric levels can be seen.

3.8 Influence of load

The abrasive wear rate is observed to increase (Figs. 6a and 6b) with an increase in load (10 to 30 N) on interaction with both speed and sliding distance.

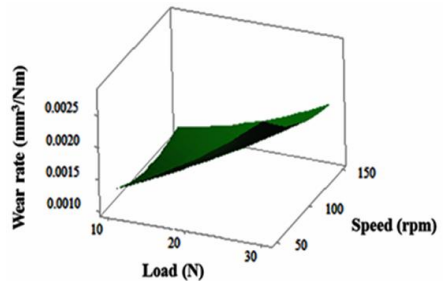

a)

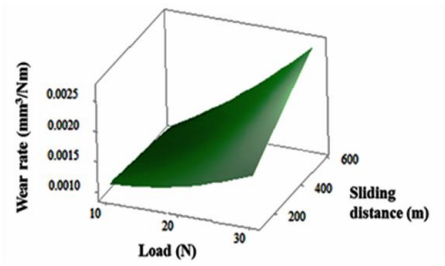

b)

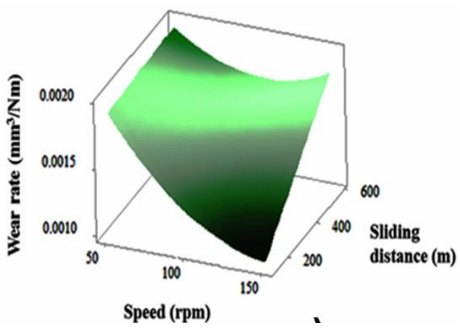

c)

Fig. 6. Surface plots for abrasion wear rate: a) Load vs Speed (Sliding distance = 353 m), b) Load vs Sliding distance (Speed = 100 rpm), and c) Speed vs Sliding distance (Load = 20 N).

At low loads (10 N), the silica sand abrasive medium freely falls between the rotating wheel and the specimen surface. These abrasive medium produce free rolling effect on the specimen and hence there is absence of crushing and ploughing effect of the silica sand abrasive medium resulting in minimum wear rate. As the load is increased 20 N the rolling effect of the silica get drastically reduced owing to the increase in contact pressure exerted at the interface of the tribosystem. This load tends to crush and compress the silica sand which in turn abrades the surface of the specimen. At highest load 30 N, abrasive wear rate increased drastically and can be attributed to the crushing of the silica sand at the initial stage of contact with the wheel and the specimen surface. Diminishing of rolling effect occurs at higher load and reduction in size of silica particles. This tends to cause more abrasion and material removal from the composites. Similar results have been reported by Antonov et al. [19] on their study on effect of temperature and load on three-body abrasion of cermets and steel.

3.9 Influence of speed

As the rotating speed of the wheel is increased from 117 to 589 rpm, the abrasion wear rate is found decrease with respect to both load and sliding distance (Fig. 6a and 6c). At 117 rpm, silica sand particles get embedded on the surface of the rotating chlorobutyl rubber wheel due to higher contact time. This embedded sand particle makes repeated contact on the surface of the specimen which results in higher wear rate. As the speed increased, number of silica sand particles getting embedded on the wheel reduces significantly owing to the low contact time with the wheel and consequently a reduction in abrasion occurs. Analogous findings were reported by Radhika and Raghu [17] in their study on Abrasive wear behavior of monolithic alloy, homogeneous and functionally graded aluminium (LM25/AlN and LM25/SiO_2) composites. Similar phenomena was also observed byGaurav Agarwal et al.[20] on their study on parametric optimization of three-body abrasive wear behavior of bidirectional and short kevlar fiber reinforced epoxy composites.

3.10 Influence of sliding distance

As the sliding distance increases from 117 m to 589 m, the abrasion wear is found to increase with respect to both load and rotating speed (Fig. 6b and 6c). During the initial stage, sharp edges of the reinforcement particles and asperities result in larger number of point contact in the specimen and the rubber wheel. Thus the, entire surface is not exposed to contact with the rubber wheel, resulting in a lower wear rate. On the other hand, as the sliding distance increases, the asperities gets smooth and extended contact with the rubber wheel for considerable distance. This results in more number of contacts of the specimen with the rubber wheel and consequently removal of more material. Similar trend was attained by Ranganatha et al. [21] on their Investigation on Three-Body Abrasive Wear of Al_2O_3 Filler on CFRP Composites.

3.11 Response optimization

Optimization of the wear process parameters using RSM was carried out through response optimiser which aids in the determination of optimum parameter to achieve minimum wear rate. In the optimizer, the highest wear rate and the target wear rate were specified as the inputs. Optimization results revealed that a load of 10 N, speed of 83 rpm and sliding distance of 117 m resulted in minimum wear rate of 0.00107 mm^3/m.

3.12 Scanning Electron Microscopy Analysis

Abraded surfaces of Al A356/ $ZrSiO_4$ composite samples under three different loading conditions of 10, 20 and 30 N at constant speed of 100 rpmand a sliding of 353

m were examined using SEM (Fig. 7a-7c) to study the influence of the significance of load on the wear behavior. Worn surface of the composites sample tested at 10 N load (Fig. 7a) shows fine scratches and shallow grooves with very minimum material removal. Low load on specimen will result in relatively less physical contact between the specimen and the rubber wheel. This leads to a rolling behavior of the abrasive particles and thus results in less ploughing action.

At 20N (Fig. 7b) and 30 N (Fig. 7c) load deeper abrasive grooves along with delamination of the surface is observed. At higher loading condition, the contact pressure between sample and wheel is high and this causes a higher degree of material removal. The silica sand particles may get embedded into the rubber wheel at higher applied loads. Abrasion caused by this inserted particles, along with freshly added particles between the wheel and specimen increases the material removal rate, similar results has been reported by Agarwal et al [22].For checking the adequacy of the RSM model, specimen tested at optimum condition was also taken for examination (Fig. 7c). This surface shows only tiny grooves with fewer scratches, as well as limited ploughing and cutting action of the abrasive medium.

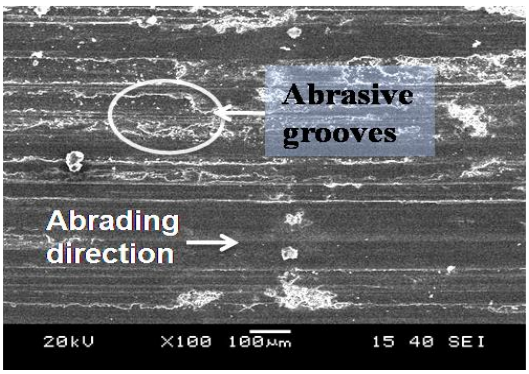

a)

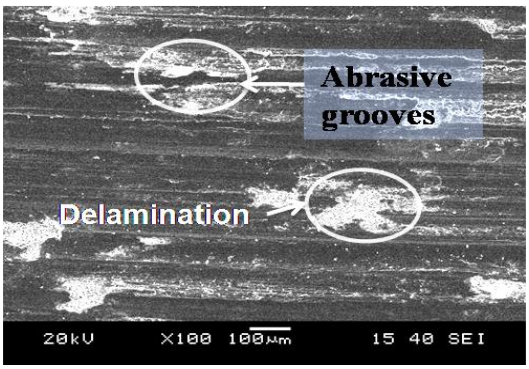

b)

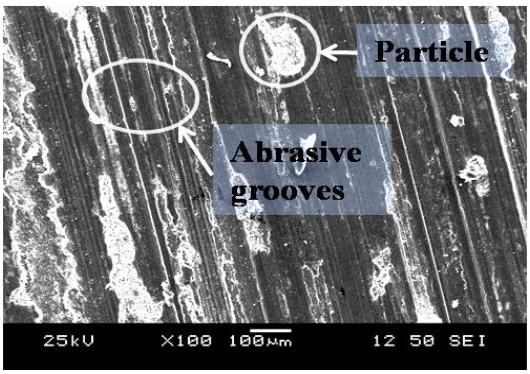

c)

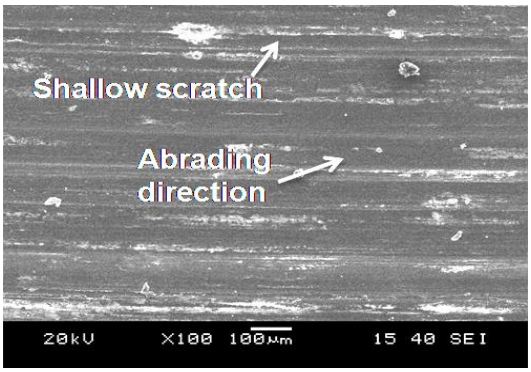

d)

Fig.7. SEM micrographs of worn out surfaces ofcomposite specimens at different conditions. a) Load = 10 N, speed = 100 rpm, sliding distance = 353 m, b) load = 20 N, speed = 100 rpm, sliding distance =353 m, c) load = 30 N, speed = 100 rpm, sliding distance = 353 m, d) SEM image of the worn out surface at optimum condition (Load = 10 N, speed= 83 rpm, sliding distance = 117 m.

This indicates that the developed model is adequate enough to predict the wear behavior of the composite. Figure 7d shows the SEM image of the worn out surface of the composite which was tested under optimum condition (Load = 10 N, speed= 83 rpm, sliding distance = 117 m. It can be observed that the specimen presents minimum grooves and shallow scratches which conclude lesser wear rate [16].

At 20N (Fig. 7b) and 30 N (Fig. 7c) load deeper abrasive grooves along with delamination of the surface is observed. At higher loading condition, the contact pressure between sample and wheel is high and this causes a higher degree of material removal. The silica sand particles may get embedded into the rubber wheel at higher applied loads. Abrasion caused by this inserted particles, along with freshly added particles between the wheel and specimen increases the material removal rate, similar results has been reported by Agarwal et

al. [22]. For checking the adequacy of the RSM model, specimen tested at optimum condition was also taken for examination (Fig. 7c). This surface shows only tiny grooves with fewer scratches, as well as limited ploughing and cutting action of the abrasive medium. This indicates that the developed model is adequate enough to predict the wear behavior of the composite. Figure 7d shows the SEM image of the worn out surface of the composite which was tested under optimum condition (Load = 10 N, speed= 83 rpm, sliding distance = 117 m. It can be observed that the specimen presents minimum grooves and shallow scratches which conclude lesser wear rate [16].

4. CONCLUSIONS

Aluminium A356/$ZrSiO_4$ MMC was successfully fabricated through stir casting process. Microstructural analysis showed uniform dispersion of $ZrSiO_4$ particles throughout the matrix. ANOVA shows that load has a significant influence on the wear rate followed by the speed and sliding distance. Sliding distance showed the least influence on abrasion rate, indicating that the material could last for longer operational cycles under optimized load conditions. Regression model developed is found to be adequate in predicting the abrasion wear of the composite through correlation of wear parameters. Surface plots revealed that abrasion rate increased both with increase in load and sliding distance while it decreased with an increase in the speed. Optimized response and found that minimum wear rate of 0.00107 mm^3/Nm is obtained for the 10 N load, 83 rpm speed and 117 m sliding distance. SEM analysis of wear tested samples showed that with an increase in load, material removal rate increased, consequently increasing the wear rate. The fabricated MMC could be used in automobile applications such as in cylinder heads, cylinder blocks and transmission cases.

Acknowledgement

We thank the University Grants Commission (Grant No. 4-4/ 2014-15, MRP-SEM/UGC-SERO) for financial support.

REFERENCES

[1] B.A. Mudasar Pasha, Keemulla Mohamed, *Taguchi Approach to Influence of Processing Parameters on Erosive Wear Behaviourof Al7034-T6 composite,* Transactions of Nonferrous Metals Society of China, vol. 27, pp. 2163-2171, 2017, doi:10.1016/S1003-6326(17)60242-5

[2] T. Satish Kumar, R. Subramanian, S. Shalini, *Synthesis, Microstructural and Mechanical Properties of Ex-Situ Zircon Particles ($ZrSiO_4$) Reinforced Metal Matrix Composites (MMCs): AReview,* Journal of Material Research and Technology, vol. 4, iss. 3, pp. 333-347, 2015, doi:10.1016/j.jmrt.2015.03.003

[3] M. Kok, *Computational Investigation of Testing Parameter Effects on Abrasive Wear Behaviour of Al_2O_3Particle-Reinforced MMCs using Statistical Analysis*, International Journal of Advanced Manufacturing Technology, vol. 52, iss.1-4, pp. 207-215, 2011.

[4] S. Das, K. Das, S. Das*, Abrasive Wear Behavior of Al 4.5 wt.%Cu/(zircon sand + silicon carbide)Hybrid Composite,* Journal of Composite Materials, vol. 43, pp. 2665–2672,2009, doi:10.1177/0021998309345305

[5] B. Praveen Kumar, B. Anil Kumar, *Microstructure and Mechanical Properties of Aluminium Metal Matrix Composites with Addition of Bamboo Leaf Ash by Stir Casting Method,* Transactions of Nonferrous Metals Society of China, vol. 27, pp. 2555-2572, 2017, doi: 10.1016/S1003-6326(17)60284-X

[6] M. Kok, *Abrasive Wear of Al_2O_3Particle Reinforced 2024 Aluminium Alloy Composites Fabricated by Vortex Method*, Composites: Part A, vol. 37, pp. 457–464, 2006.

[7] T. Satish Kumar, R.Subramanian, S. Shalini, P.C. Angelo, *Microstructure, Mechanical Properties and Corrosion Behaviourof Al-Si-Mg Alloy Matrix/Zircon and Alumina Hybrid Composite*, ForschungimIngenieurwes, vol. 79, pp. 123-130, 2015, doi: 10.1007/s10010-016-0198-5

[8] J. Singh, A. Chauhan, *Fabrication Characteristics and Tensile Strength of Novel Al2024/SiC/Red Mud Composites Processed via Stir Casting Route,* Transactions of Nonferrous Metals Society of China, vol. 27, pp. 2573-2586, 2017, doi: 10.1016/S1003-6326(17)60285-1

[9] S. Das, V. Udhayabanu, S. Das, K. Das, *Synthesis and Characterization of Zircon Sand/Al-4.5 wt%Cu Composite Produced by Stir Casting Route*, Journal of Materials Science, vol. 41, pp. 4668–4677, 2006, doi: 10.1007/s10853-006-0056-1

[10] P. Sharma, D. Khanduja, S. Sharma, *Dry Sliding Wear Investigation of Al6082/Gr Metal Matrix Composites by Response Surface Methodology*,Journal of Materials Research and Technology, vol. 5, pp. 29-36, 2016, doi: 10.1016/j.jmrt.2015.05.001

[11] N. Radhika, K. Sai Charan, *Experimental Analysis on Three Body Abrasive Wear Behaviour of Stir Cast Al LM 25/TiC Metal Matrix Composite*, Transactions of the Indian Institute of Metals, vol. 70, iss. 9, pp. 2233–2240, 2017, doi: 10.1007/s12666-017-1061-6

[12] N.Ch. Kaushik, R.N. Rao, *Effect of Grit Size on Two Body Abrasive Wear of Al 6082 Hybrid Composites Produced by Stir Casting Method*, Tribology International, vol. 102, pp. 52-60, 2016, doi: 10.1016/j.triboint.2016.05.015

[13] N. Natarajan, A.A. Moorthy, R. Sivakumar, M.Manojkumar, M.Suresh, *Dry Sliding Wear and Mechanical Behavior of Aluminium/Fly Ash/Graphite Hybrid Metal Matrix Composite using Taguchi Method,* International Journal of Modern Engineering Research, vol. 2, pp. 1224-1230, 2012.

[14] M. Kok, *Prediction and Optimisation of Abrasive Wear Model for Particle Reinforced MMCs using Statistical Analysis*, Materials Research Innovations, vol. 15, iss. 5, pp. 366-372, 2011.

[15] S. Singh, M. Garg, N.K. Batra, *Analysis of Dry Sliding Behavior of Al_2O_3/B_4C/Graphite Aluminum Alloy Metal Matrix Hybrid Composite using Taguchi Methodology*, Tribology Transactions, vol. 58, iss. 4, pp.758-765,2015, doi: 10.1080/10402004.2015.1015757

[16] N. Radhika, *Analysis of Three Body Abrasive Wear Behaviour of Centrifugally Cast Aluminium Composite Reinforced with Ni Coated SiC using Taguchi Technique*,Tribology in Industry, vol. 40, iss. 1, pp. 81-91, 2018.

[17] N. Radhika, R. Raghu, *Abrasive Wear Behavior of Monolithic Alloy, Homogeneous and Functionally Graded Aluminum (LM25/AlN andLM25/SiO_2) Composites*, Particulate Science and Technology, pp. 1-11, doi: 10.1080/02726351.2016.1199074

[18] J. Nampoothiri, B. Raj, K.R. Ravi, *Role of Ultrasonic Treatment on Microstructural Evolution in A356/TiB_2In-Situ Composite*, Transactions of the Indian Institute of Metals, vol. 68, pp. 1101-1106, 2015, doi: 10.1007/s12666-015-0653-2

[19] M.N. Antonov, I. Hussainova, R. Veinthal, J. Pirso, *Effect of Temperature and Load on Three-Body Abrasion of Cermets and Steel,* Tribology International, vol. 46, pp. 261-268, 2012, doi: 10.1016/j.triboint.2011.06.029

[20] G. Agarwal, A. Patnaik, R.K. Sharma, *Parametric Optimization of Three-Body Abrasive Wear Behavior of Bidirectional and Short Kevlar Fiber Reinforced Epoxy Composites,* International Journal of Engineering Research and Applications, vol. 2, pp. 1148-1167, 2012.

[21] S.R. Ranganatha, H.C. Chittappa, D. Tulsidas, *Investigation on Three-Body Abrasive Wear of Al_2O_3 Filler on CFRP Composites,* International Journal of Advanced Engineering Research and Studies, vol. 2, iss. 3, pp. 83–85, 2013.

[22] G. Agarwal, A. Patnaik, R.K. Sharma, *Comparative Investigations on Three-Body Abrasive Wear Behavior of Long and Short Glass Fiber-Reinforced Epoxy Composites,* Advanced Composite Materials, vol. 23, pp. 293–317, 2014, doi: 10.1080/09243046.2013.868661